Int J Adv Manuf Technol (2018) 94:2333–2341
DOI 10.1007/s00170-017-0981-y

ORIGINAL ARTICLE

Characterization of direct selective laser sintering of alumina

E. M. Fayed[1] · **A. S. Elmesalamy**[1] · **M. Sobih**[2] · **Y. Elshaer**[1]

Received: 30 May 2017 / Accepted: 14 August 2017 / Published online: 8 September 2017

Abstract The last three decades have seen a growing trend towards high-temperature ceramic parts processed with selective laser sintering technology, due to recent development of laser processing facilities. The aim of the present research is to understand the effect of the laser sintering parameters (power and laser scanning speed) on the quality of the sintered layer characteristics (layer surface roughness, layer thickness, layer deformation, and vector/line width). Moreover, the influence of the laser sintering parameters on layer physical properties and microstructure are investigated. Based on the obtained results, the physical properties for fabricating sintering layer can be improved. The results show that maximum density of the sintered ceramic layers are of 3.54 g/cm^3 and minimum porosity of 4.34%. The hardness of the higher physical properties was measured with Vickers micro hardness and was found to be 1682 Hv with standard deviation 113.

Keywords Ceramic laser sintering · Selective laser sintering · Laser processing

✉ A. S. Elmesalamy
aselim@mtc.edu.eg

E. M. Fayed
eslamfayed2009@gmail.com

[1] Mechanical Design and Production Department, Military Technical College, Cairo, Egypt

[2] Mechatronics Systems Engineering Department, October University for Modern Sciences and Arts (MSA), Giza, Egypt

1 Introduction

Selective laser sintering (SLS) is an additive manufacturing technique where parts are fabricated layer by layer. Powder layers are deposited by a roller or a scraper. Laser beam is used as a heat source to heat and sinter the deposited powder layer locally according to predetermined geometries. The sequence of powder deposition and laser scanning is repeated until the part is completed [1].

SLS is one of the most popular rapid prototyping and manufacturing processes for complex components with diverse material types from metal, plastic, ceramic, etc. [2]. Three-dimensional arbitrary-shaped components can be produced through additive laminated material process by using computer-aided design and computer-aided manufacture (CAD/CAM). Accordingly, SLS can reduce the design time and total cost compared to conventional sintering methods [2]. Theoretically, any powders which are bonded together due to heating can be used as raw materials for SLS. This technology has a wide range of applications and has received considerable critical concern by different industries owing to the diversity of SLS forming material [2].

Ceramics are considered a promising alternative to the common metallic materials for the most industries [2]. Alumina (Al_2O_3) is one of the most important ceramic materials. The diversity of applications of alumina derives from its distinctive properties [3]. It has a high-melting temperature of 2040 °C, and it is very stable chemically. This leads to developed as the supplementary material in a lot of high-temperature components, catalyst substrates, and biomedical implants. Alumina can be used to improve the bearings and cutting tools manufacturing [4] due to its high hardness, strength, and abrasion resistance.

F. Klocke et al. and C. Ader [5] studied the effect of the laser power, laser scanning speed, and hatch spacing on the

laser-sintered part density and surface roughness. The results showed that increasing the laser power leads to an increase in the density of the specimen and surface roughness. However, increasing the laser scanning speed leads to decrease the density and improve the surface finish. Decreasing the hatch spacing leads to an overall increase in part density and increase the surface roughness.

Wei Wang et al. [2] determined the optimal parameters of scanning speed and laser power for $Al_2O_3/ZrO_2/SiO_2$ mixture sintering by using three patches, then investigated the effect of laser power and laser scanning speed on the laser-sintered part density and sintering width. It was found that the width of laser-sintered vectors is wider at higher laser power with decreasing laser scanning speed. Moreover, increasing of the laser power leads to increase the part density, but after certain limit oversintering occurs. The dimensions of oversintered parts do not meet the requirement and few bubbles exist in the interior of the parts which decrease its density.

Shishkovsky et al. [6] used SLS to synthesize a porous refractory ceramics from mixture of zirconium dioxide, aluminum, and/or alumina. The dependency of the monolayer thickness and deformation on the laser power and laser scanning speed was explored. It was concluded that increasing the laser power with decreasing laser scanning speed results in thicker monolayer. At the same time, deformation was observed that reaches critical value under high power and low speed, which was not suitable for sintering.

Hsiao-chuan Yen et al. [7] established a systematic method for measuring the width and depth of the scan line on thin ceramic layer sintered with laser scanning furthermore to obtain the optimum scanning process parameter (laser power and scanning speed) to achieve better surface quality and higher strength. They concluded that the laser power is directly proportional to layer surface temperature, line depth, and line width. Moreover the laser scanning speed is inversely proportional to the layer surface temperature, line depth, and line width.

Xiaoyong Tian [8] used laser sintering for porcelain slurry to study the dependence of properties of ceramic components (mechanical properties and microstructure) on the process parameters. Four key factors in direct laser sintering process were investigated: laser power, scan speed, hatch spacing, and layer thickness. The results include that low laser power (50 W), large hatch spacing (0.6 mm), and high scan speed (85 mm/s) always produce relative high-bending strength of the final ceramic components (34 ± 4.9 MPa) after being post sintered in the furnace (1425 ~ 1475)°C.

J.I. Packard et al. [9] manufactured 3D airplane models, letter bars, etc. from mixtures of alumina powder. They investigated that laser energy density (laser power, beam spacing, and the laser scan speed) plays an important role in the SLS process. Then alumina ceramic parts were obtained by post sintering parts at 1600 °C for binder burnout. This resulted in a ceramic with a relative density of 88% and average flexural strength of 255 MPa.

Peter Regenfuß et al. [10] used several novel techniques for ceramic sintering by laser beam. Compact bodies as well as coatings of alumina were treated with CO_2- and Nd: YAG-laser beam. AlN was processed with an argon ion laser. Decreasing sintering time and selectivity are considered the main advantages of using high-power density sintering techniques. Average value of Vickers hardness for ceramic samples exceeds 2000 Hv processed using laser sintering. These values are very high compared to samples processed by conventional furnace-sintering technique.

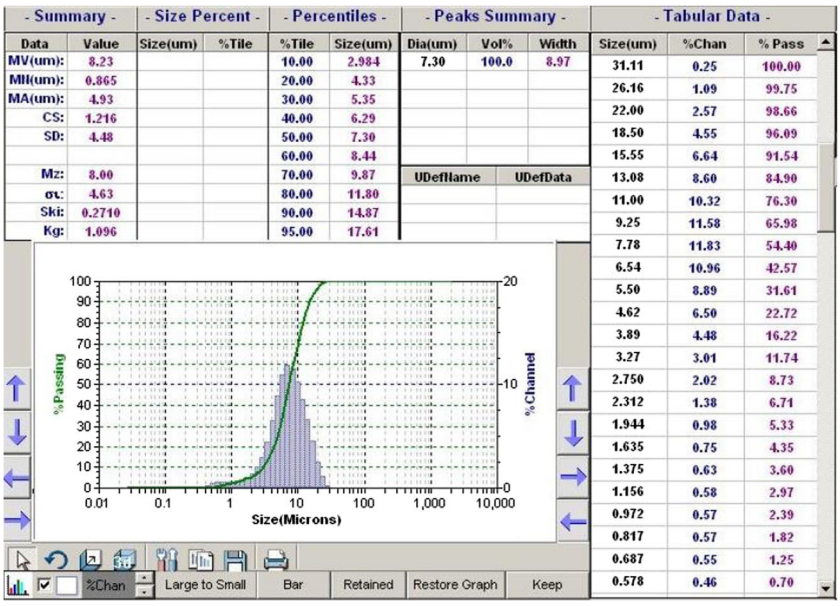

Fig. 1 The obtained histograms for as received alumina powder

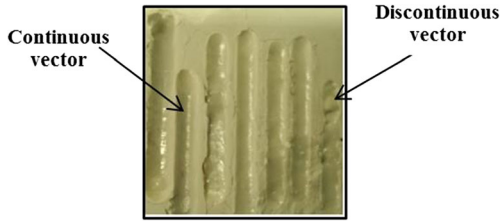

Fig. 2 Optical images showing the continuous and discontinuous vectors

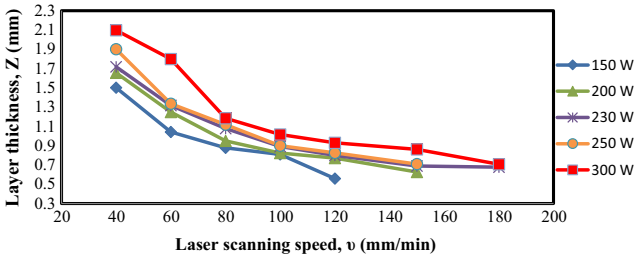

Fig. 4 Laser sintering vectors thickness (Z) vs. laser scanning speed *v*

Although the preceding researchers investigated the influence of laser power and laser scanning speed, a complete understanding of the influence of these parameters and their interaction in detail to obtain high-quality sintered layer is still a point of weakness.

The main objective of this work is to understand the effect of significant laser sintering parameters (laser power and laser scanning speed) and their interaction on the quality of the laser sintering monolayer (surface roughness, thickness, deformation, and vector line width), physical properties (density and porosity), and mechanical properties of ceramic laser-sintered components. The experimental methodology has been described and the results of the experiment have been assessed and discussed. The work results were extended to establish a statistical model to control and optimize the laser sintering parameters [11]. It is also hoped that this work will provide a foundation for future work involving wear resistance investigation and numerical modeling for the process.

2 Experimental study

2.1 Sample preparation

High purity alumina (98.8% Al_2O_3 from TAIMICRON) with a mean particle size of 8 μm was used in this study. The histograms of the average grain size of the as received alumina powder were determined using the Microtrac S3500 particle size analyzer as shown in Fig. 1. It is observed that the particle size distributions ranged from 0.5 to 30 μm. But the major average particle size is 8 μm which represents 60% from the powder. The result of this particle size distribution is the key for improving packing density and consequently the sintered sample density. Small particles improve not only the surface quality but also the sintering process itself. They need less energy for melting comparing to large particles. Density of the sintered sample will be improved by forming molten particles that fill up the porous structure.

To prepare the sample for sintering process, the powder was placed on a surface of mild steel substrate. Compaction die assembly was used with pressure 50 MPa. It was pressed into square layer of 50 × 50 and 3 mm thickness by using uniaxial press (SANTEC 100 ton hydraulic press, India).

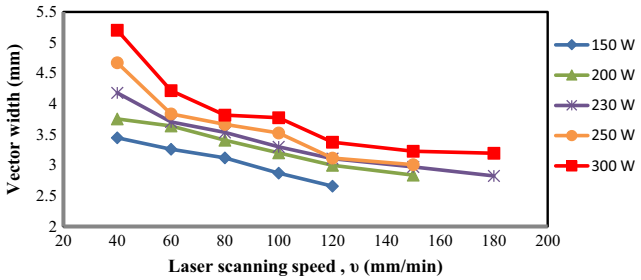

Fig. 3 Laser sintering vectors width vs. laser scanning speed *v*

2.2 Laser sintering of ceramic samples

A pulsed Nd:YAG laser machine (LUMONICS JK 702 LASER MACHINE) is used for laser sintering process. The Nd:YAG laser has a maximal power of 330 W with a wavelength of 1064 nm and 140 mm focal length. The minimum beam diameter is 0.92 mm at 10 mm below the gas nozzle tip. The minimum beam diameter was measured by trigger a low laser power beam with 20 W on a sensitive thin film. The laser beam path is moved over the powder surface according to the predefined 2D parallel lines using 3D CNC table. The laser sintering process is carried out using a defocused beam of 1.68 mm diameter to cover a big area in a small time. According to screening set of experiments, the height of the laser nozzle plane is adjusted to be at 30 mm above the powder surface with defocused distance of 20 mm to minimize the formation of plasma which could scatter the powder particles [12]. Above this plane, the alumina laser sintering was not accomplished and below this plane, the plasma formation increased according to screening experiments.

The operating window for speed and laser power is determined from the screening experiments. Accordingly, ranges of

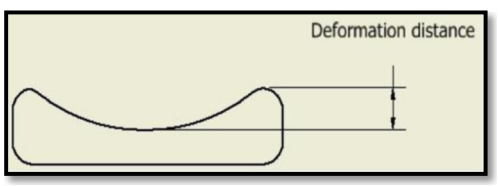

Fig. 5 Scheme represents the surface deformation

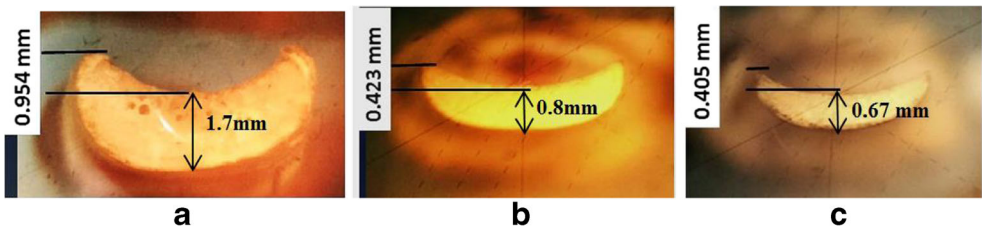

Fig. 6 Optical microscope images of three cross-section monolayers sintered at different scanning speeds (**a**, **b**, **c**) 40, 120, and 180 mm/min, respectively, at laser power of 230 W

laser power and scanning speed containing the successful sintering samples were between 150 and 300 W and 40–180 mm/min respectively. The pulse width and repetition rate are constant for all average powers. But the average power changes with change of pulse height (%) due to its significant effect.

The influences of control factors (laser power and laser scanning speed) on the output responses were investigated within the limits of the acceptance window. The output responses of the process includes the vector width, layer thickness, surface deformation, surface roughness, density, porosity, and microstructure.

Line width and thickness for each layer were measured by using Mitutoyo toolmaker microscope. The surface roughness (Ra) of the laser-sintered layer was determined using surface roughness meter (Mitutoyo SJ.201). The average value of ten measurements was considered for each monolayer. Physical properties in terms of bulk density were determined using a liquid displacement technique (Archimedes) via a weight measurement.

3 Results and discussion

3.1 Effect of laser power and scanning speed on sintered single vectors

3.1.1 Vector continuity

The existence of continuous vectors (full pass sintered successfully) and interrupted vectors (partially sintered) at different laser powers and laser scanning speeds is observed clearly, as shown in Fig. 2. Continuous vectors are sintered at scanning speed range 40:180 mm/min, at the power range 150:300 W. When the laser scanning speed is higher than 180 mm/min and/or the laser power is lower than 150 W, discontinuity of the sintered vector is obvious. This is due to insufficient energy/unit length delivered to ceramic powder to cause sintering. However, when the laser scanning speed is less than or equal to 40 mm/min and the laser power is greater than or equal to 300 W, irregular vectors are obvious.

The increased temperature due to high power leads to increase the width of the heat-affected zone and decrease the surface tension coefficient and viscosity of the molten phase; consequently, the vectors will be interrupted.

3.1.2 Sintered vector width

Figure 3 summarizes the width of laser sintering monolayer vectors at different laser powers (150 to 300) W and different scanning speeds (40 to 180) mm/min. The sintered vector width is directly proportional to laser power and inversely proportional to laser scanning speed, as shown in Fig. 3. Increasing the laser power and/or decreasing the scanning speed leads to increase the amount of energy delivered to the ceramic layer. Temperature is increased and hence the volume of the sintered particle. This results in increasing the width of the melted pool.

3.2 Effect of laser power and laser scanning speed on the layer thickness

Based on the performed experiments, Fig. 4 represents the dependency of the layer thickness (Z) on laser scanning speed (υ) and laser power (P). It is observed that sintered layer is thicker by increasing the laser power and decreasing laser

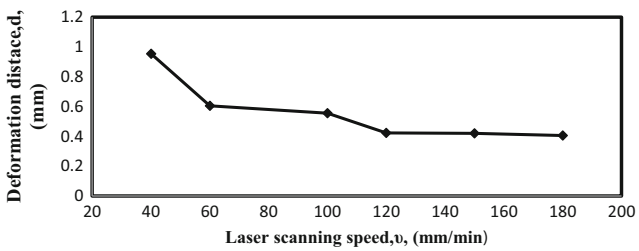

Fig. 7 Deformation distance, d, of the monolayer sintered vs. laser scanning speed, υ, at laser power 230 W

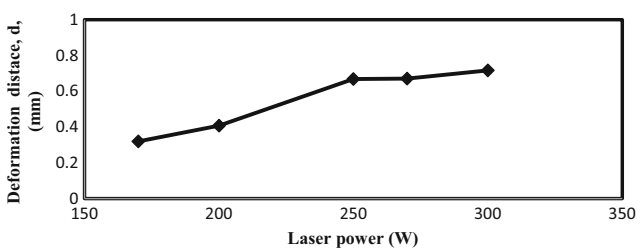

Fig. 8 Deformation distance, d, of the monolayer sintered vs. laser power at laser scanning speed 80 mm/min

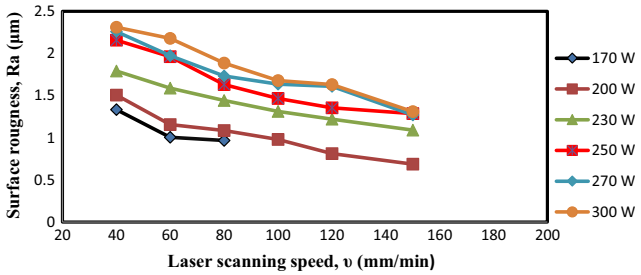

Fig. 9 Surface roughness of the monolayer sintered vs. laser scanning speed υ

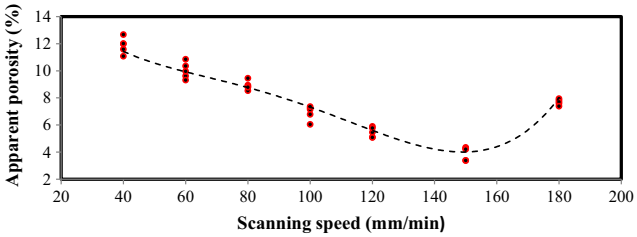

Fig. 11 Apparent porosity percentage vs. scanning speed at laser power 230 W

scanning speed. This is due to the increase of the amount of energy delivered to ceramic powder surface by increasing the laser power and/or decreasing the laser scanning speed. That leads to increase the volume of sintered powder, (increasing the width of the melted pool), consequently increases the sintered layer thickness.

3.3 Effect of laser power and scanning speed on the layer surface deformation

Surface deformation is the distance between the upper point and lower point on the upper sintered surface as shown in Fig. 5. Surface deformation will equal to zero if the upper surface is flat, i.e., deformation surface distance will be zero. Deformation in the ceramic monolayer is accompanied with sintering process and its increase leads to difficulty in multilayer (building up) process [6]. Figure 6 shows the optical microscope images for the surface deformation of the sintered layer cross section using laser power 230 W and different scanning speeds 40, 120, and 180 mm/min. Figure 7 represents graphically deformation distance of the sintered layer as a function of laser scanning speed at laser power 230 W. It is observed that the surface deformation is inversely proportional to laser scanning speed. While Fig. 8 shows the opposite effect for the surface deformation as a function of laser power at laser scanning speed 80 mm/min, where, the surface deformation is directly proportional to laser power at constant laser scanning speed. It was observed that the sintering process is unstable if the laser power increased more than a certain critical value that prevent the lamination and fabricating 3D parts. The increased pressure at point of interaction between the laser beam and the center point of the upper surface of the sintered layer due to laser shockwave is considered the main reason for the layer deformation. Also, the difference in thermal cycle between the lower and upper surface of the sintered part, as the upper surface is rapidly heated then rapidly cooled than the lower surface. Moreover, the change of temperature profile of the sintered vector leads to a change in the surface tension coefficient as well as melting viscosity between upper and lower surface of the sintered vector.

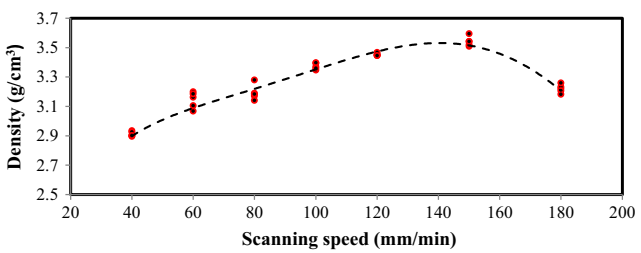

Fig. 10 Average density vs. scanning speed at laser power 230 W

3.4 Effect of laser power and laser scanning speed on the layer surface roughness

Figure 9 represents graphically the relationship between the surface roughness (Ra) of the laser-sintered layer and the scanning speed as well as laser powers. It was found that increasing the laser power and/or decreasing scanning speed leads to an increase in the surface roughness. The amount of energy that delivered to unit length of the ceramic powder will increase by increasing laser power and/or decreasing laser scanning speed. Consequently the sintered particles tend to form larger spherical structures due to their effort to reduce the free enthalpy by optimizing the ratio between the area of free surfaces and the related volume. This will lead to form a coarse-sintered surface that increases the surface roughness. Moreover, increasing the scanning speed leads to decrease the interacting time between laser and sintered surface, which improve the surface roughness by minimizing the possibility of plasma formation.

3.5 Effect of laser power and laser scanning speed on physical properties of sintered layer

Density and porosity are very important physical properties of the sintered ceramic parts. The influence of the laser sintering parameters on the density and porosity has been investigated and explained here after.

Figures 10 and 11 show the density and apparent porosity, respectively, of the laser-sintered samples as a function of laser scanning speed at laser power 230 W. It is observed that at

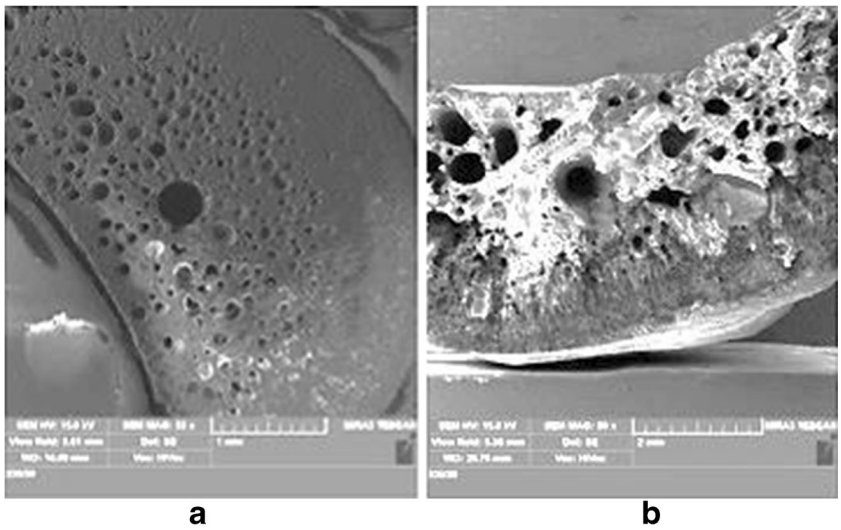

Fig. 12 SEM micrograph of laser-sintered layer made using at P = 230 W and v = 40 mm/min: (**a**) polished cross section (**b**) fracture surface

laser power of 230 W, increasing laser scanning speed from 40 to 150 mm/min leads to an increase in average density from 2.93 to 3.54 g/cm^3, and to decrease in apparent porosity of the sintered layer from 11.1 to 4.34%. But after a scanning speed of 150 until 180 mm/min, the density of the sintered part decreases to be 3.219 g/cm^3 and the apparent porosity increases to be 7.83%. Since at very low scanning speed, instability of the molten powder and trapped bubbles results from unstable key hole formation. This is mainly due to an increase in the duration of the interaction time between the laser beam and surface which caused further increasing in delivered energy and temperature that caused oversintering. These results are in a good agreement with others work [2, 13]. Oversintering is a common phenomenon in laser sintering. It is mainly due to high temperature at high laser power or long sintering time (low laser scanning speed). It deteriorates the final product quality. The dimensions of oversintered parts do not meet the manufacturing requirements and a few bubbles exit in the interior of the parts which decrease the density as shown in Fig. 12 [2]. Furthermore, at very high speed, the duration of the interaction between the laser beam and surface decreased. Insufficient energy delivered to ceramic powder which consequently caused not complete sintering and decrease the density [5].

Figures 13 and 14 show the density and apparent porosity, respectively, of the laser-sintered samples as a function of laser power at laser scanning 150 mm/min. It is observed that at laser scanning speed of 150 mm/min, increasing laser power from 200 to 230 W leads to an increase in average density from 3.37 to 3.54 g/cm^3, and to decrease in apparent porosity of the sintered layer from 5.81 to 4.34%. Increasing the laser power to 300 W, leads to decrease the density of the sintered part to 3.31 g/cm3 and increases the apparent porosity to be 8%. More energy is delivered into the powder by increasing laser power. That will lead to enhance the bonding mechanism between particles. Consequently, the density is increased and the porosity of the sintered sample is decreased. Further increasing laser power leads to oversintering as shown in Fig. 12.

The maximum obtained density was 3.54 g/cm^3, while minimum apparent porosity was 4.34%. These results were achieved at laser power 230 W and laser scanning speed 150 mm/min. These values represent approximately 90% from the theoretical density of the alumina 3.96 g/cm3. According to our application, higher density and lower porosity was the best demand, so we considered the process parameter which achieve the maximum physical properties is the optimum parameter (230 W and 150 mm/min).

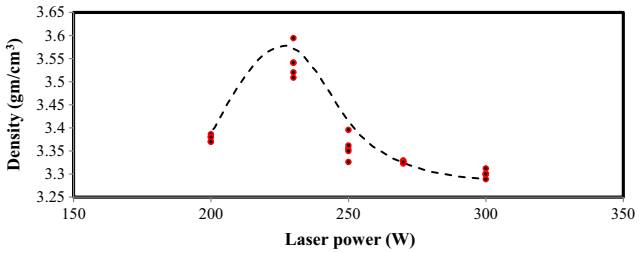

Fig. 13 Average density vs. laser power at laser scanning speed 150 mm/min

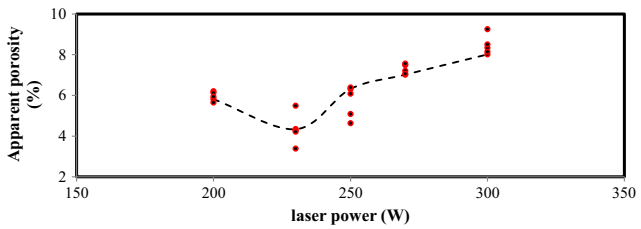

Fig. 14 Apparent porosity percentage vs. laser power at laser scanning speed 150 mm/min

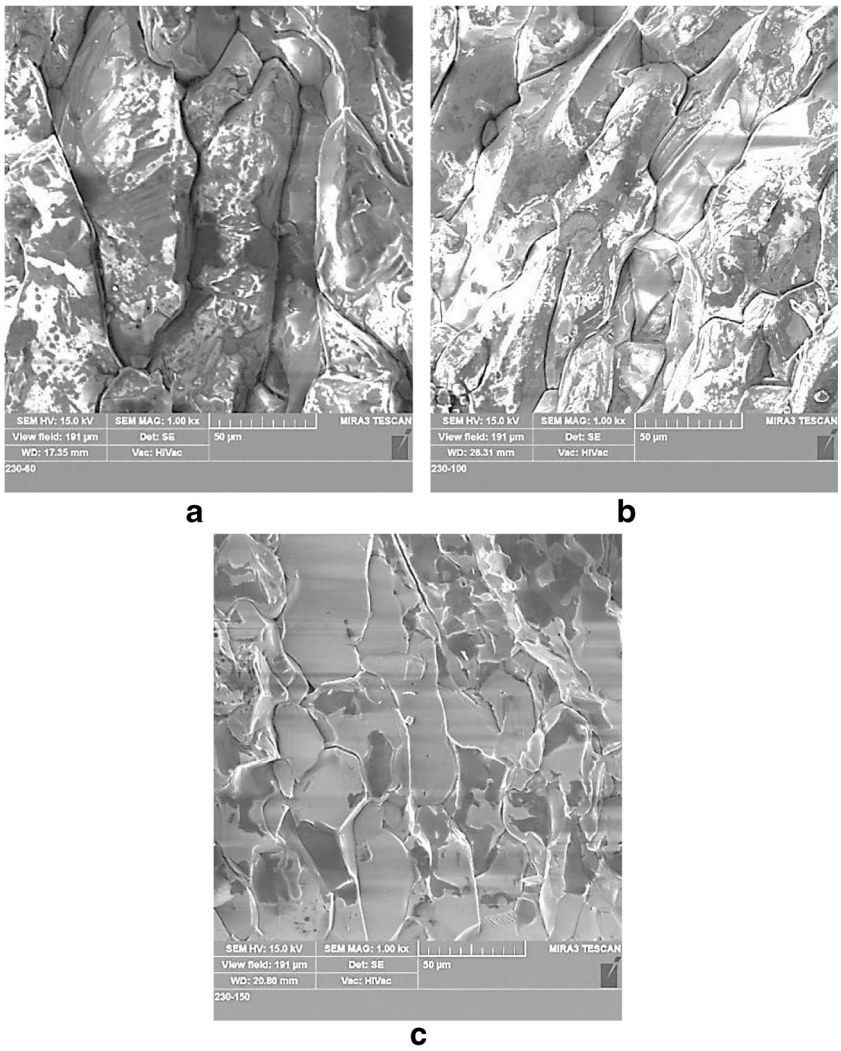

Fig. 15 SEM micrographs of a cross section of laser-sintered alumina made using 230 W power and different speeds. (**a**) 60 mm/min. (**b**)100 mm/min. (**c**)150 mm/min

3.6 Microstructure evaluation

Microstructure and both physical and mechanical properties of the sintered layer are dependent. A lot of works have been focused on the microstructure investigations of ceramics. Controlling the sintering parameters and the composition and of ceramic materials are considered the key factors to improve morphology and enhance the material properties.

All samples were prepared for SEM evaluation. The first step is cutting the sintered sample by using diamond micro-cutter wheel and then cold mounting for all specimens cross section. Samples were rough polished by using abrasive grinding sheet from size 600 to 120 μm gradually. Then, fine polishing was accomplished by using diamond abrasive and cleaning by using acetone and methanol. Samples were coated with metal film to be conductive.

Figure 15 shows SEM micrographs of laser-sintered sample by using laser power of 230 W and different scanning speeds 60, 100, and 150 mm/min. It is observed that the decrease in the laser scanning speed at power 230 W leads to increase in the grain size (grain growth). Because decreasing laser scanning speed results in increase in the duration of the interaction between the laser beam and surface, more energy is delivered to the powder. Hence, particles tend to form larger spherical structures due to their effort to reduce the free enthalpy by optimizing the ratio between the area of free surfaces and the related volume. The formed coarse microstructure affects the physical and mechanical properties of the sintered part [14]. Based on the results obtained from the physical properties (density and porosity) at section 3.5, the most desirable physical properties can be obtained by applying laser power 230 W and laser scanning speed 150 mm/min. This is cleared in a microstructure evaluation as shown in Fig. 15c where minimum grain size and low porosity optimization of the sintering process was investigated and assessed in detail in our work for statistical modeling for the process [11].

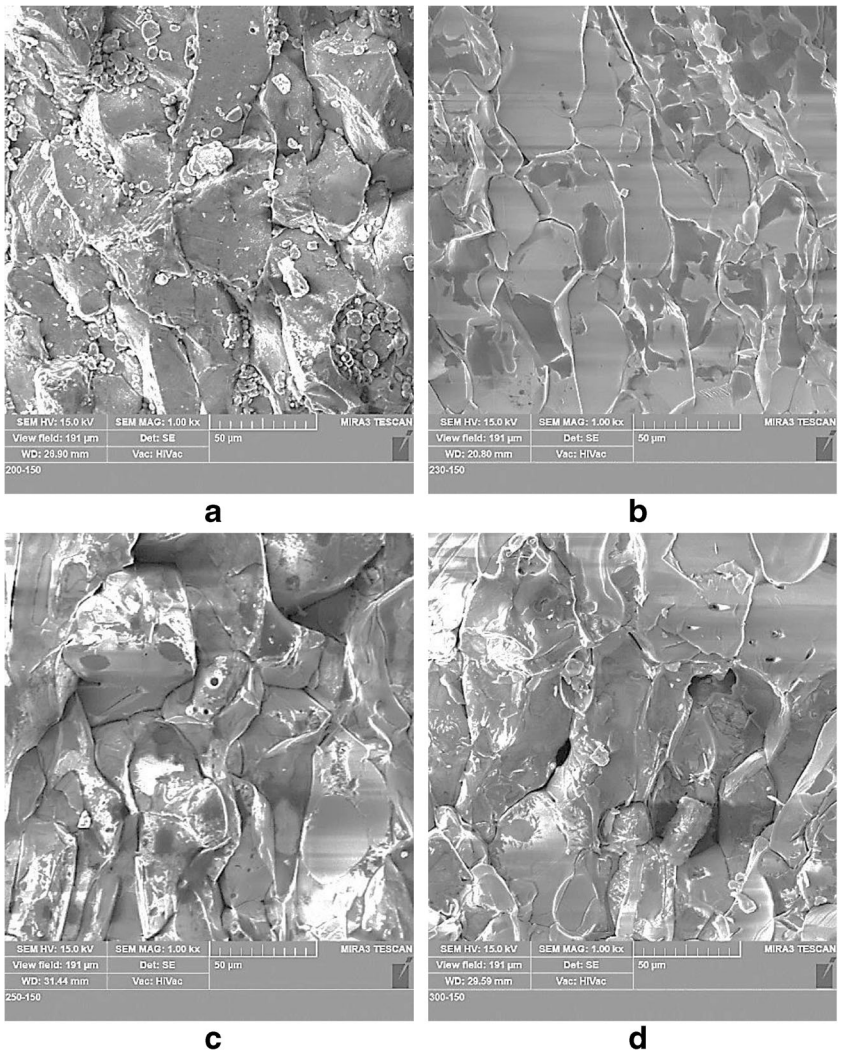

Fig. 16 SEM micrographs of a cross section of laser-sintered alumina at scanning speed 150 mm/min and different powers: (**a**) 200 W (**b**) 230 W (**c**) 250 W (**d**) 300 W

Figure 16 shows SEM micrographs of laser-sintered sample by using different laser powers 200, 230, 250, and 300 W at laser scanning speed of 150 mm/min. It is observed that the increase in the laser power at laser scanning speed 150 mm/min leads to increase in the grain size (grain growth). Since increasing laser power/energy results in particles tend also to form larger spherical structures due to their effort to reduce the free enthalpy by optimizing the ratio between the area of free surfaces and the related volume.

Finally, it can be concluded that from Figs. 15 and 16, the optimum microstructure can be obtained by applying laser power 230 W and laser scanning speed 150 mm/min that insures the results of the physical properties testing at section 3.5.

3.7 Micro hardness test

The hardness of the laser-sintered ceramic sample that achieves maximum physical properties is measured using a Vickers diamond micro hardness testing machine (BUEHLER OMNIMET MHT). The applied load is 500 g and magnification value is ×50.

The measured Vickers micro hardness of the alumina layer that fabricated by the optimum laser parameters is shown in the Table 1.

The results of the Vickers hardness of optimal sample were compared with the previous works of P. Figiel et al. [15]. Alumina was obtained using conventional free-sintering process and the non-conventional methods (microwave sintering

Table 1 The measured Vickers micro hardness of laser-sintered alumina at power of 230 W and scanning speed of 150 mm/min

Sample	Applying load (g)	Hardness (Hv)	St. dev.
Laser-sintered alumina at P = 230 W and υ = 150 mm/min	500	1682.4	113

and spark plasma sintering). Vickers hardness of Al_2O_3 ceramics was measured and it was found that the hardness of the samples sintered by conventional free sintering was 1200 HV while the hardness of the samples sintered by spark plasma sintering was 1600 HV.

It can be concluded that using of non-conventional sintering such as spark plasma sintering and laser sintering results in better mechanical properties due to limited available time for grain growth [15].

4 Conclusion

Ceramic laser sintering has been successfully conducted with a 330 W pulsed Nd: YAG laser. The present investigation has clearly demonstrated the significant effect of laser sintering power and laser scanning speed on the sintered monolayer surface roughness, monolayer thickness, monolayer deformation, vector line width, density, porosity, and hardness.

- Increasing of the laser power and/or decreasing of the laser scanning speed leads to increasing the width of the sintered vector, increasing of the monolayer thickness, increasing the monolayer deformation, increasing the monolayer surface roughness, increasing the grain size, and increasing of the density of the sintered part until certain value for laser power and/or laser scanning speed the density decreased due to oversintering.
- Sintering parameters could be optimized to improve both physical and mechanical properties. The maximum density of sintering samples was 3.54 g/cm^3 and minimum porosity 4.34%. The results can be obtained by applying laser power 230 W and laser scanning speed 150 mm/min.
- Further increasing/decreasing for these two control parameters (laser power and scanning speed) will lead to lower physical properties which can be used for different application such as filters.
- The micro hardness of the best physical properties was 1682 Hv with standard deviation 113.

References

1. Shahzad K, Deckers J, Kruth J-P, Vleugels J (2013) Additive manufacturing of alumina parts by indirect selective laser sintering and post processing. J Mater Process Technol 213:1484–1494
2. Wang W, Ma S, Fuh J, Lu L, Liu Y (2013) Processing and characterization of laser-sintered Al2O3/ZrO2/SiO2. Int J Adv Manuf Technol 68:2565–2569
3. Shackelford JF, Doremus RH (2008) Ceramic and glass materials. Springer, New York
4. Elshaer Y (2003) Fracture of ceramic/metal laminates. Ph.D. dissertation, Manchester Institute of Science and Technology
5. Klocke F, Ader C (2003) Direct laser sintering of ceramics. State of the Art Report, Fraunhofer Institute of Production Technology IPT, Aachen, Germany, pp. 447–455
6. Shishkovsky I, Yadroitsev I, Bertrand P, Smurov I (2007) Alumina–zirconium ceramics synthesis by selective laser sintering/melting. Appl Surf Sci 254:966–970
7. Yen H-C, Chiu M-L, Tang H-H (2009) Laser scanning parameters on fabrication of ceramic parts by liquid phase sintering. J Eur Ceram Soc 29:1331–1336
8. Tian X (2010) Rapid prototyping of ceramics by direct laser sintering. Papierflieger-Verlag
9. Liu Z, Nolte JJ, Packard J, Hilmas G, Dogan F, Leu M-C (2007) Selective laser sintering of high-density alumina ceramic parts. In: Proceedings of the 35th international MATADOR conference, pp 351–354
10. Reinecke A-M, Regenfuß P, Nieher M, Klötzer S, Ebert R, Exner H (2007) Laser beam sintering of coatings and structures. Laserinstitut Mittelsachsen e.V. an der Hochschule Mittweida, Germany
11. Fayed E, Elmesalamy A, Sobih M, Elshaer Y (2016) Multi-objective optimization for alumina laser sintering process. Lasers Manuf Mater Process 3:174–190
12. Elmesalamy ASE (2013) Narrow gap laser welding of 316L stainless steel for potential application in the manufacture of thick section nuclear components. Ph.D. dissertation, The University of Manchester, Faculty of Engineering and Physical Sciences
13. Elmesalamy A, Li L, Francis J, Sezer H (2013) Understanding the process parameter interactions in multiple-pass ultra-narrow-gap laser welding of thick-section stainless steels. Int J Adv Manuf Technol 68:1–17
14. Klocke F, Ader C (2003) Direct laser sintering of ceramics. In: Solid freeform fabrication symposium. pp 447–455
15. Figiel P, Rozmus M, Smuk B (2011) Properties of alumina ceramics obtained by conventional and non-conventional methods for sintering ceramics. J Achiev Mater Manuf Eng 48:29–34